

Development of Multi-Material-Joint Made of Copper-Coated FRP and Steel by Innovative Technology Fusion

Jana Gebauer¹⁾, Rico Drehmann²⁾, Kevin Eisner²⁾, David Kupke²⁾, Andrés Fabian Lasagni^{1,3)}

- 1) Business Unit Cutting and Joining, jana.gebauer@iws.fraunhofer.de, Fraunhofer Institute for Material and Beam Technology, Winterbergstrasse 28, 01277 Dresden, Germany
- 2) Materials and Surface Engineering Group, Institute of Materials Science and Engineering, rico.drehmann@mb.tu-chemnitz.de, keisner3004@gmail.com, david_kupke@web.de, Chemnitz University of Technology, Erfenschlager Str. 75, 09125 Chemnitz, Germany
- 3) Faculty of Mechanical Engineering, Institute for Manufacturing Technology, andres_fabian.lasagni@tu-dresden.de, Technische Universität Dresden, George-Bähr-Str. 3c, 01069 Dresden, Germany

Keywords

Climate Chamber Test, FRP-Metal-Joint, Low-Temperature Soldering, Pulsed Laser Processing, Wire Arc Spray Deposition

Abstract

Several technologies have been developed to join metal and polymer, such as adhesive bonding, clinching or screwing. These have disadvantages in terms of creep tendency of the adhesives or structural damage to the fiber-reinforced plastic (FRP).

An innovative process chain consisting of laser pre-treatment of the FRP before metallization by thermal spraying and the subsequent low-temperature soldering process enable a reliable multi-material bond, without structural damage either of the FRP or the metal part. In addition to a rough joining surface, the laser pre-treatment enables the deep interlocking of the thermally sprayed copper coating with the carbon fibre-reinforced plastic (CFRP) substrate. After the adhesion strength of the copper-coated CFRP could be doubled to 18 MPa compared to grit-blasting, this hybrid was joined to a steel counterpart with a soft solder BiSnAg1 using infrared heating. Additionally, the hybrid achieved a flexural stress of 1128.0 MPa in a 4-point-bending test without coating impairment. The multi-material joint achieved up to 15.5 MPa in the tensile shear test. During fatigue testing, the specimens withstood 5.000.000 load cycles at a maximum stress of 15 MPa and a mean stress of 8.6 MPa without any measurable structural damage. After salt water aging, the joining zone remained unaffected.

1 Introduction

Weight reduction is necessary to increase the range of Battery Electric Vehicles. In an attempt to make the vehicle body lighter, various lightweight construction concepts and lightweight technologies have been investigated. Challenges remain in successfully and efficiently combining dissimilar materials such as fiber-reinforced plastics (FRP) and metals.

Currently, adhesive joints, mechanical joining elements or inserts are often used to join FRP to metal. Adhesive bonding allows a very homogeneous stress distribution, but also represents an irreversible joining technique [1]. Mechanical joining elements might allow reversible joining of different materials, but for FRP, the fiber structure is damaged and local stress concentrations occur, so that higher material thicknesses become necessary [2]. The inclusion of inserts enables the joining of metals and FRP without damaging the fibers. Due to the integration during the manufacturing process, this joint is also non-separable and expensive to produce. Soldering is another way to join different materials. However, it is only suitable for metallic materials. Thus, in order to use it for joining FRP with metallic materials, it is necessary to metallize the composite material with a metallic coating.

Currently, the joining of FRP and metals by soldering is still largely unexplored. First investigations were carried out by Winkelmann et al. who joined a sandwich sheet consisting of a both-side steel-sheet covered FRP core with another steel sheet using the soldering alloy SnCu3. The amount of thermal energy input during the joining process is one of the most important parameters to prevent delamination within the sandwich [3]. Zhou et al. improved the mechanical properties of magnesium alloy-based hybrid fiber-metal laminates (FML) by using solder interlayer. Bonded with a magnesium alloy solder, a higher interlaminar and tensile performance could be achieved, than traditional Mg-FMLs, bonded with epoxy resin [4].

A very effective method for producing metallic coatings directly onto the polymer surface is demonstrated by thermal spraying technologies [5, 6]. In advance of the coating process, the FRP surface undergoes a pre-treatment process. This is usually carried out using grit-blasting in order to roughen the surface and thus ensure adhesion to the substrate. However, this also results in damage to the fibers close to the surface caused by the sharp and highly accelerated blasting particles [7]. Liu et al. investigated the shear tensile strength of wire arc sprayed coatings on a carbon fiber reinforced thermoset polyimide whose substrate surface was treated by the grit-blasting process under 4 bar pressure. The zinc coating achieved a maximum shear bond strength of 10.5 MPa and the aluminum coating 7.5 MPa [5]. Wang et al. achieved adhesion strengths up to 13.8 MPa, applying a zinc-aluminum coating on a mechanically blasted carbon fiber-reinforced plastic (CFRP) [8]. Ganesan et al. observed a mechanical adhesion of the coating to the rough, grit-blasted surface. Compared to the thermally pre-treated surface, this led to an increase of the bond strength to 2.2 MPa (50–60 μm coating thickness) and 1.2 MPa (120–130 μm coating thickness), respectively [10].

Due to the high heat input during the soldering process, special demands are made on the adhesive strength of the sprayed coating on the substrate. For this reason, the adhesive strength should be as high as possible. In contrast to mechanically blasted structures, laser structuring enables a reproducible and defined surface design. There are several studies demonstrating that a laser-structured surface can improve the bond strength for various joining technologies, such as adhesive bonding, injection molding, laser joining and more [10-14]. Laser pre-treatment of CFRP substrates before thermal spraying of a metal layer has been investigated for the first time by Gebauer et al. [15-17]. Two laser structures were compared to grit-blasted CFRP substrates, as a reference, before applying a wire flame sprayed aluminum coating. In the pull-off test, a cross-like structure was shown to increase the bond strength above 40 % to 12.4 ± 5.5 MPa compared to the grit-blasted reference samples. Furthermore, the bonding strength in pull-off tests of laser pre-treated CFRP samples coated with 80Ni20Cr by atmospheric plasma spraying achieved an average adhesion strength of 20.3 ± 2.7 MPa. The combination of a cross-like structure with laser roughening even resulted in composite failure and an adhesion strength of 28.5 ± 0.8 MPa [16].

In this work, different laser structures following recent investigations by Gebauer et al. [18] are applied to the CFRP substrate with the objective of increasing the adhesion strength of the wire arc sprayed coating to the CFRP substrate. The results were compared to the state-of-the-art pre-treatment mechanical blasting. Subsequently, the coated CFRP is joined to a metallic counterpart by a low-temperature soldering process.

2 Materials and methods

2.1 Materials

The substrate material used in this study was a thermoset CFRP (SIGRAPREG® C U 600-0/SD-E501/33%) with a thickness of 1.85 mm consisting of an epoxy resin with unidirectional oriented carbon fibers (from SGL Carbon, Wiesbaden, Germany). The fiber volume content is specified as 67 %. Whereas the decomposition temperature of the composite is 873 K, the maximum operating temperature of the epoxy is 543 K. At temperatures above, thermal decomposition of the epoxy matrix occurs. A softening of the epoxy can arise at temperatures above the glass transition temperature of 383 K. For the pull-off tests, round samples with a diameter of 25 mm were used. The samples for the shear tensile tests have an area of 100 mm \times 25 mm. All test samples were produced by water jet cutting.

The coating material used was a copper wire (> 99.8 % Cu) with 1.6 mm diameter (from GTV Verschleißschutz GmbH, Luckenbach, Germany). To perform the shear tensile test, a metallic

counterpart cut out of an aluminum sheet (EN AW6082) with the volume of 100 mm × 25 mm × 2 mm was utilized. The coated CFRP samples and the grit-blasted aluminum counterparts were joined with an overlap area of 12.5 mm × 25 mm. FM 1000 adhesive film (HTK Hamburg GmbH, Hamburg, Germany) was used to produce the test samples for shear tensile and pull-off tests. In order to prevent oxidation of the coating, the samples were cured in an electric oven at 433 K for 60 min in argon atmosphere.

For the mechanical testing of the multi-material joints, a steel counterpart was soldered onto the copper-coated CFRP parts. The properties of the used materials are summarized in Table 1.

Table 1: Properties of utilized materials

Material	Name	Thickness in mm	Tensile strength in MPa	Young's modulus in GPa
CFRP	SIGRAPREG® C U-600-0/ SD-E501/33%	1.9	2000	130
Aluminum sheet	EN AW-6082	2.0	300–350	70
Steel sheet	1.0226	2.0	270–500	210
Solder	BiSn42Ag1	0.2	70	-

As explained in the introduction, grit-blasting is considered state of the art for surface pre-treatment prior to thermal spraying. For this reason, grit-blasted CFRP substrates were used to show reference values in the mechanical testing.

2.2 Innovative technology fusion

The multi-material bond of CFRP and a aluminum counterpart was achieved by three process steps as shown in Fig. 1. Firstly, the CFRP was laser-structured by a pulsed laser system before a metal coating was applied by a wire arc spraying process. Finally, after applying a thin layer of low-temperature solder on the metal coating, the metallized CFRP part was joined with the metal counterpart by infrared heating.



Figure 1: Process chain consisting of laser pre-treatment of CFRP, thermal spray deposition of a copper coating, low-temperature soldering to a steel counterpart to produce a three-dimensional multi-material joint; © Fraunhofer IWS

Figure 1 shows the composite formation of three-dimensional components to depict an industrial-scale application of a multi-material-knot, for example in a car body. The mechanical tests were performed on flat specimens.

2.2.1 Surface pre-treatment of CFRP substrates

For laser structuring, the Nd:YAG laser Avia NX40 from Coherent, offering a maximum laser power of 20 W, operating with a wavelength of 355 nm and a pulse duration of 30 ns, was used. The laser roughening (R) structure avoided untreated areas with smooth epoxy material. The combination of laser roughening and a trench-like structure (R+TS) was chosen to enlarge the effective joining surface by

additional trenches with a distance of 300 µm in fiber direction and perpendicular to it. The trenches had a trench depth of approx. 100 µm (in fiber direction). The optical setup of the pulsed laser system included a lens with a focal length of 160 mm producing a spot diameter of approx. 20 µm.

Grit-blasted (GB) specimens using EK24 corundum at 0.2 MPa pressure, 100 mm distance and 70° angle, were used as reference samples in mechanical testing.

2.2.2 Metallization of CFRP substrates

Copper coatings were deposited by means of wire arc spraying, using a VisuArc350 inverter, a Schub5 gun (both Oerlikon Metco Europe GmbH, Kelsterbach, Germany) and a six-axis robot (KUKA AG, Augsburg, Germany). Nitrogen was used as process gas. In order to prevent thermal degradation of the CFRP substrate, which has a maximum operating temperature of 543 K, each deposition cycle was followed by a 5 minute cooling break. The spray parameters are shown in Table 2.

Table 2: Thermal spraying parameters (for the determination of the flow rate see [19])

Current in A	Voltage in V	Spraying distance in mm	Traverse speed in m/s	Gas pressure in MPa	Flow rate in m ³ /h
80	40	150	1	0.6	142.6

2.2.3 Low-temperature soldering of metallized CFRP substrate to metal counterpart

Soldering was chosen for joining CFRP and metal, because, as opposed to conventional joining processes such as clinching or riveting, the fibers of the CFRP are not damaged. The temperature sensitivity of the thermoset CFRP matrix material had to be taken into account when choosing a suitable solder material and soldering process. Thus, only solders with a melting temperature below 543 K were considered, focussing on soft solders based on tin or bismuth. The eutectic alloy of 43 wt.-% tin and 57 wt.-% bismuth has a melting temperature of only 411 K and proved particularly suitable. The addition of 1 wt.-% silver prevents the formation of the brittle intermetallic phase Cu₆Sn₅, which improves the formability of the solder. Therefore, the commercially available solder alloy BiSn42Ag1 from Haines & Maassen Metallhandelsgesellschaft mbH (Bonn, Germany) was used for the low-temperature soldering process. Since the solder was delivered as ingots, it had to be rolled into 0.2 mm thin foils for the soldering process.

In order to achieve an optimum flow behaviour of the solder alloy, a homogeneous heating of the joining zone is needed. In preliminary investigations, three different heat sources were tested – hot plate, induction heating and infrared radiation. Infrared radiation resulted in the most homogeneous heat input and reproducible process control, thus the joining test rig shown in Fig. 2 was used for the further experiments. The test rig consists of a short-wave omega round tube infrared radiator made of quartz glass with a gold reflector with a maximum power of 1850 W regulated by the power controller Heratron type CB1x25 P both supplied from Heraeus Nobelight GmbH (Hanau, Germany). The process parameters are displayed in Table 3.

Table 3: Soldering process parameters

Radiator intensity in %	Distance from radiator to surface in mm	Heating time in s	Solder thickness in µm
60	40	100	200

As shown in Fig. 2, the steel sheet was placed above the CFRP in order to absorb most of the emitted infrared radiation. The solder alloy melts due to the heat conduction of the steel sheet while the thermal load on the CFRP is kept below the degradation temperature of the thermoset matrix.

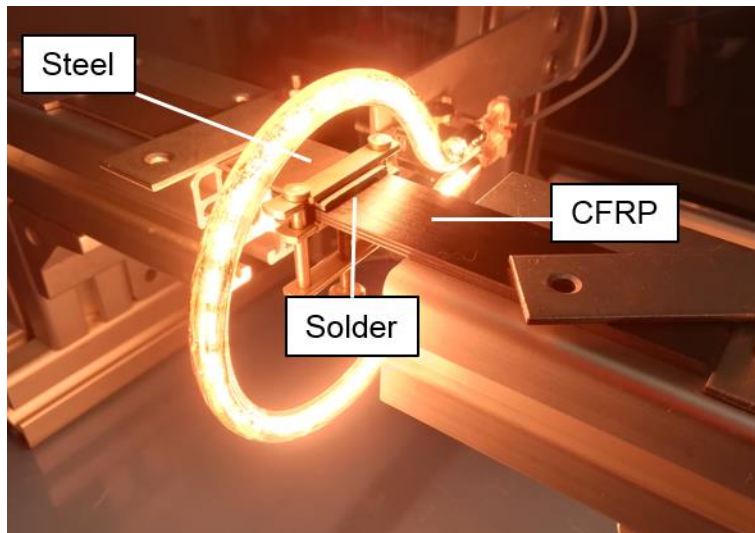


Figure 2: Joining test rig with infrared radiation as heat source

2.3 Characterization methods

The substrate surfaces were analyzed before the coating process using the confocal laser scanning (CLS) microscope VK-X200 from Keyence (Osaka, Japan). The roughness R_a of all surface pre-treatments was determined according to DIN EN ISO 4287. The CLS enabled a contactless measurement not affecting the filigree and contact-sensitive surface structures.

By using the scanning electron microscope (SEM) JSM-6610LV from JEOL (Akishima, Japan), the topography of the generated surface structures was analyzed. Furthermore, detailed characterization of the joining and fracture zone after mechanical testing was performed by metallographic cross-sections prepared by standard metallographic techniques and analyzed with the SEM LEO 1455VP (Zeiss, Jena, Germany) and Olympus GX51 inverted microscope (Olympus Europa SE & Co. KG, Hamburg, Germany).

The adhesion strength of the coating was investigated using in pull-off and shear tensile tests, five samples each. The pull-off test was implemented according to DIN EN ISO 14916, using a tensile and compression testing machine Zwick UPM 1475 from Zwick/Roell (Ulm, Germany), equipped with a 100 kN load cell. The crosshead speed was set to 1 mm/min. Eight test samples were tested for each surface structure. The tensile shear strength of the coating and the multi-material bond was determined by the shear tensile test on the basis of the DIN EN 1465, using the tensile and compression testing machine Zwick Z020 from Zwick/Roell, equipped with a 20 kN load cell. The crosshead speed was set to 1 mm/min. Six test samples were used to verify the influence of each surface structure on the tensile shear strength of the thermally sprayed copper coatings, while five multi-material joints were tested to determine the tensile shear strength of the CFRP-steel bond.

The determination of the coating adhesion under bending load was qualitatively investigated by means of the 4-point bending test using the above-mentioned universal testing machine Zwick UPM 1475 with a testing speed of 1 mm/min. The specimen geometry and the test setup were selected on the basis of DIN EN 843-1 and DIN EN 843-2 with a substrate geometry of 45 mm in length and 10 mm in width. The thickness is specified as 2 mm. The thickness of the purchased CFRP sheets, from which the substrates were taken by waterjet cutting, was about 1.85 mm. The coating of the substrates was carried out based on the previously obtained findings with the parameters from Table 2. The number of layers was selected so that the coating thickness was about 100 μm . The bending stiffness and flexural strength were calculated on the basis of DIN EN 14125. The number of specimens was five.

An important criterion for assessing the fatigue strength of a bonded joint is the cyclic bond strength. With the aid of a resonance pulsator RUMUL Testronic (Russenberger Prüfmaschinen AG, Neuhausen am Rheinfall, Switzerland) with a 20 kN load cell, the shear tensile specimens were tested under tension-tension load with an R ratio of 0.14. A maximum stress of 15 MPa was chosen for the cyclic tests, according to the maximum shear tensile strength which was achieved in the shear tensile tests. The mean stress was set to 8.6 MPa. Termination criteria of the tests were a maximum number of load

cycles $N_D = 10^6$ (specimen is considered fatigue-resistant) or a frequency drop of 1 Hz (specimen has failed). One selected sample was even subjected to $5 \cdot 10^6$ load cycles.

In a salt spray test according to DIN EN ISO 9227, a 5 % sodium chloride solution was evaporated in a chamber. The three samples inside were exposed to this environment for 1000 hours at 308 K.

3 Results and discussion

3.1 Pre-treatment and metallization of CFRP

In Figure 3, SEM images of the pre-treated CFRP surfaces are shown. The laser-roughened (Fig. 3a) and the grit-blasted surface (Fig. 3c) indicate a highly irregular surface. While the laser roughening left a relatively flat surface, the grit-blasting process generated a highly pronounced unevenness. Furthermore, corundum blasting particles were embedded in the soft polymer matrix of the CFRP. Fiber damage is only evident after grit-blasting due to the impact of the highly accelerated blasting particles, as already explained in the introduction. Figure 3b shows the combination of laser roughening and grid structure. The grid structures have a trench distance of 300 μm and a depth of 100 μm with a trench orientation (with respect to the fiber direction) of $0^\circ/90^\circ$.

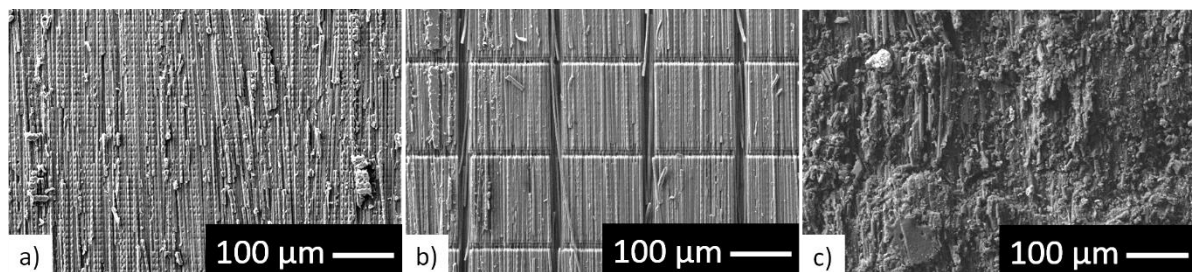


Figure 3: SEM images of a) laser-roughened substrate, b) laser-roughened substrate with trench-like structure and c) grit-blasted substrate

The laser-roughened surface had the lowest roughness R_a of $4.2 \pm 0.7 \mu\text{m}$, followed by the grit-blasted surface with $8.5 \pm 1.1 \mu\text{m}$. The combination of laser roughening and trench-like structure achieved the highest roughness of $9.5 \pm 0.9 \mu\text{m}$.

The results of the pull-off and tensile shear testing of the copper-coated CFRP are shown in Fig. 4. In pull-off testing, the laser-roughened specimens achieved the lowest adhesion strength with $6.9 \pm 1.8 \text{ MPa}$, followed by the grit-blasted samples with $9.1 \pm 2.1 \text{ MPa}$ and $18.1 \pm 2.0 \text{ MPa}$ by the combined structured ones. With increasing surface roughness, the adhesive strength under tensile stress, perpendicular to the surface, increased.

In the tensile shear testing, the grit-blasted samples achieved the lowest adhesion strength with $10.0 \pm 0.9 \text{ MPa}$, followed by the laser-roughened specimens with $11.1 \pm 2.5 \text{ MPa}$ (Fig. 4). Obviously, the shattered fibers on the surface of the substrate of the grit-blasted specimens provide a lower resistance to the tensile shear stress than the intact fibers of the laser-roughened structure, despite the fact that the roughness is only half. The highest adhesion strength, similar to the pull-off testing, was reached by the combined structure at $18.2 \pm 2.1 \text{ MPa}$. Beside the highest roughness value, this structure offered a massively enlarged interface area due to the 100 μm deep trenches. Furthermore, the fiber ends exposed in the trenches provide undercuts for the coating material, as already investigated in Gustke et al. [19]. Moreover, the trench-like structure provides sufficient anchorage points for the copper coating to shrink onto the substrate during the cooling process after thermal spraying.

Consequently, by the combination of laser roughening and trench-like structure, the adhesion strength could be doubled in the pull-off test and was increased up to 182 % under tensile shear load, compared to the state-of-the-art technology grit-blasting.

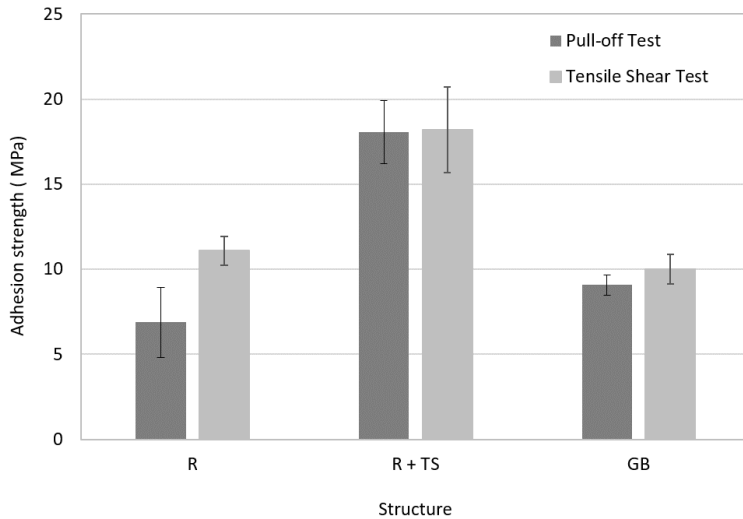


Figure 4: Adhesion strength of copper-coated CFRP samples as determined by pull-off and tensile shear tests (R = laser-roughened, R + TS = laser-roughened + trench-like structure, GB = grit-blasted)

The mechanical performance of the three surface conditions was furthermore tested in the 4-point-bending test. Table 4 shows the achieved fracture stresses including information about possible coating failure. As a reference, the average fracture stress of untreated plain CFRP specimens is listed. The plain CFRP failed under fracture stress of 1196.7 ± 45.1 MPa. A similar fracture stress was achieved by the metallized laser-roughened samples with 1194.1 ± 24.9 MPa and 1180.4 ± 36.6 MPa for the copper-coated grit-blasted specimens. The hybrids with laser roughening and trench-like structure reached an average fracture stress of 1128.0 ± 96.3 MPa. The only surface condition that did not exhibit coating failure were the specimens with the combined laser structure. A closer comparison of fracture stresses is not meaningful given the delamination failure in the substrate, visible in Figure 5.

Table 4: Fracture stresses in 4-point-bending test

	Fracture stress in MPa	Standard deviation in MPa	Coating failure
Untreated	1196.7	45.1	-
R	1194.1	24.9	yes
R+TS	1128.0	96.3	no
GB	1180.4	36.6	yes

Figure 5 shows the fracture pattern, exemplarily for the pre-treatments grit-blasting and laser roughening in Fig. 5a and for the combined laser structure in Fig. 5b.

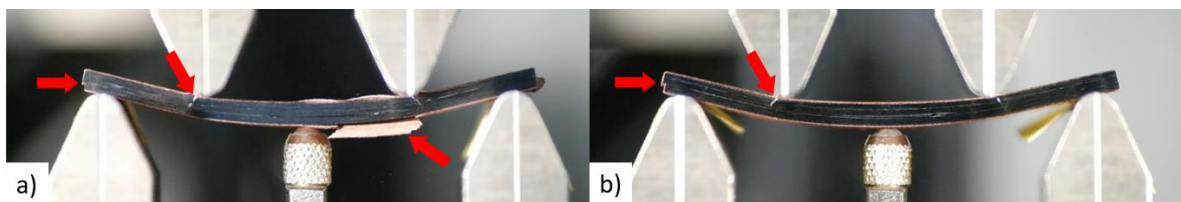


Figure 5: Failure behaviour after 4-point-bending test for a) grit-blasted and b) laser-roughened and trench-like-structured CFRP; red arrows show failure spots such as in the contact area between specimen and testing stamps, internal delamination of the specimen or coating delamination

Despite the similar fracture stresses of the differently pre-treated specimens above 1100 MPa, the specimens exhibited different failure patterns. Firstly, cracks, starting from the contact area with the testing stamps, are weakening the hybrid. In the immediate vicinity of this cracks, the coating bulges slightly. Later on, all specimens, regardless of their pre-treatment, showed internal delamination in the CFRP substrate. Up to this point, the failure behaviour is similar for all conditions. However, only with the grit-blasted and the laser-roughened samples, the copper coating finally flakes off on the tensile side, while the samples with trench-like structures did not show notable signs of coating delamination.

3.2 Multi-material joint

In the following, the mechanical properties of multi-material joints were investigated, whereby the laser-structured and copper-coated CFRPs were joined to steel sheets. This was realized by means of soldering in the infrared joining test rig described in chapter 2.2.3. The results of the subsequent tensile shear tests are shown in Fig. 6.

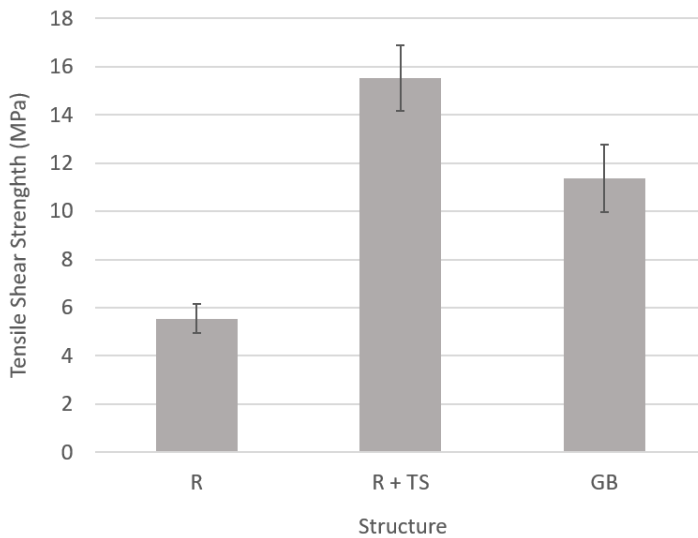


Figure 6: Tensile-shear strength of a copper-coated CFRP with different surface pre-treatments (R = laser-roughened, R + TS = laser-roughened + trench-like structure, GB = grit-blasted) soldered to a steel counterpart

The highest shear tensile strength by far was again shown by the compounds using a CFRP substrate that was roughened by laser and additionally provided with a trench-like structure (Fig. 6). These specimens reached values of 15.5 ± 1.3 MPa, while the grit-blasted specimens with 11.4 ± 1.4 MPa and the laser-roughened specimens with 5.5 ± 0.6 MPa achieved significantly lower shear tensile strengths.

The reason for these significant differences was revealed in the fracture patterns of the shear tensile specimens observed for laser-roughened and combined structured specimens. In the compounds where a laser-roughened CFRP substrate was used, complete delamination of the thermally sprayed copper coating occurred (Fig. 7 top). If the laser-roughened substrates were additionally provided with a trench-like structure, this led to a mixed adhesive-cohesive failure, as evidenced by the remains of the copper coating on the CFRP substrate (Fig. 7 bottom).

This observation correlates very well with the roughness values of the pretreated CFRP substrates. While the substrates roughened by laser had a roughness R_a of only $4.2 \mu\text{m}$, R_a of the substrates with trench-like structure was $9.5 \mu\text{m}$ (perpendicular to the fiber direction). This increased roughness enables better mechanical interlocking of the thermally sprayed copper coating to the substrate and thus higher shear tensile strength of the multi-material joint.



Figure 7: Fracture surfaces of two wire arc-sprayed copper coatings on CFRP with different surface pre-treatments (top: laser roughening, bottom: R+TS) soldered to a steel sheet

3.3 Climate chamber testing of multi-material joint

Climatic chamber tests were carried out to verify the practical suitability of the multi-material joints in terms of corrosion behavior. The test was done with one sample, which was pre-treated with laser-roughening and trench-like structure. Figure 8 shows the cross-section of a soldered CFRP-steel joint after 1000 h climate chamber testing. While the upper steel surface exhibits some severe corrosive attack (oxide formation), the joining zone remains unaffected. Neither the CFRP substrate nor the copper coating show any signs of corrosion-induced changes (Fig. 8b). The protruding BiSn42Ag1 solder prevents the corrosion medium from entering the joining zone thereby protecting the structural integrity of the compound.

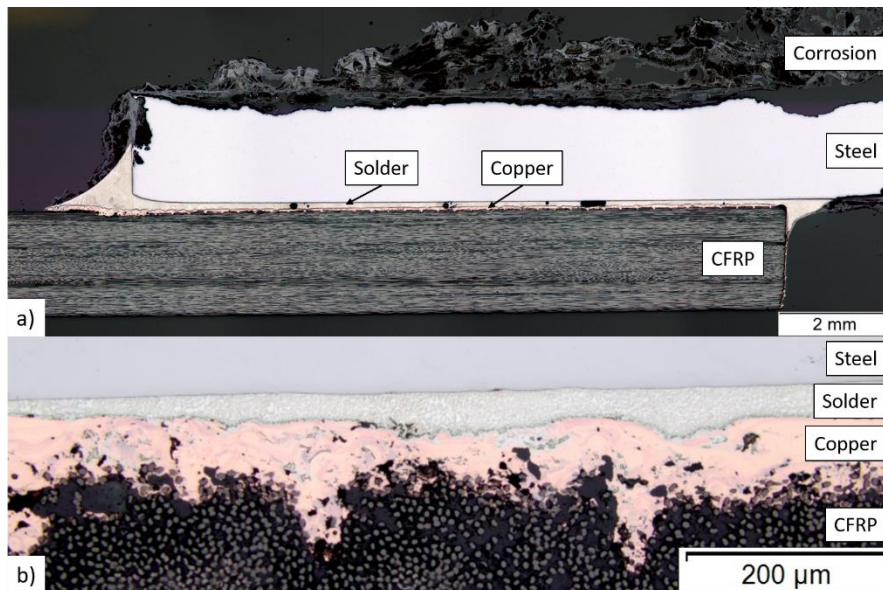


Figure 8: Cross section of multi-material joint after climate chamber testing a) as an overview and b) the joining zone in detail

4 Conclusion

Carbon fiber-reinforced epoxy was pre-treated with pulsed laser radiation to enable an optimum adhesion base for the copper coating applied by wire arc spraying. Compared to the reference method, grit-blasting, the bond strength was increased by laser structuring from 10.0 MPa to 18.2 MPa in the

tensile shear test and from 9.1 MPa to 18.1 MPa in the pull-off test. This massive increase in adhesion strength was due to a number of factors. The laser structure, which consists of a laser roughening and a trench-like structure, provides a higher roughness of the substrate surface as well as a greatly increased interface area. The trenches play a special role: The melt-tough metal particles penetrate into the depths of the laser structure and form countless undercuts as they solidify. During the cooling process, the metal shrinks to the square islands between the trenches, thus forming not only a form fit but also a force fit. All these effects lead to an increase of 200 % of the adhesive strength of the copper coating on CFRP.

Based on this metallized CFRP, a steel counterpart was soldered to the copper-coated substrate with the help of a BiSn42Ag1 low-temperature solder and an infrared heat source. Laser structuring with trench-like structures again proved to be the best solution showing the maximum shear tensile strength among all investigated multi-material joints, which can be attributed to the strong bonding between the thermally sprayed copper coating and the CFRP substrate. The CFRP-steel compounds furthermore exhibited an excellent corrosion resistance in a salt spray test according to DIN EN ISO 9227. While the steel surface was subjected to severe corrosive attack, the CFRP substrate and the joining zone with the copper coating and the BiSn42Ag1 solder remained unaffected even after 1000 h test time. The investigations demonstrate the practical suitability of the produced multi-material joints and the clear superiority of laser-structured, thermally coated CFRP substrates over conventional grit-blasting.

Acknowledgements

This project was funded under contracts 100343527/100343532 via Sächsische Aufbaubank by the European Structural Funds EFRE and by the Free State of Saxony.

References

- [1] Habenicht, G.: Kleben. Berlin, Heidelberg: Springer, 2019.
- [2] Schürmann, H.: Konstruieren mit Faser-Kunststoff-Verbunden. Berlin, Heidelberg: Springer, 2007.
- [3] Winkelmann, R.; Kilian, A.; Bürkner, G.; Alaluss, K.: Entwicklung einer Technologie zum thermischen Fügen beschichteter Stahl/Kunststoff/Stahl-Verbundwerkstoffe – Spray-Brazing. Forschungsvorhaben P 1073 / S024/10214/14.
[https://www.google.com/url?sa=t&rct=j&q=&esrc=s&source=web&cd=&ved=2ahUKEwjQNm8rLzAhWKGKewKHf_CQsQFnoECAQQAQ&url=https%3A%2F%2Fwww-docs.b-tu.de%2Ffg-fertigungstechnik%2Fpublic%2Fdokumente%2F\(5\)%2520Forschungsvorhaben%2520P%25201073.pdf&usq=AOvVaw30kjO_fuaAQkWDyBVMGKbO](https://www.google.com/url?sa=t&rct=j&q=&esrc=s&source=web&cd=&ved=2ahUKEwjQNm8rLzAhWKGKewKHf_CQsQFnoECAQQAQ&url=https%3A%2F%2Fwww-docs.b-tu.de%2Ffg-fertigungstechnik%2Fpublic%2Fdokumente%2F(5)%2520Forschungsvorhaben%2520P%25201073.pdf&usq=AOvVaw30kjO_fuaAQkWDyBVMGKbO)
- [4] Zhou, X.; Zhao, Y.; Chen, X.; Liu, Z.; Li, Z.; Fan, Y.: Fabrication and mechanical properties of novel CFRP/Mg alloy hybrid laminates with enhanced interface adhesion. *Materials and Design* 197 (2021). doi: 10.1016/j.matdes.2020.109251
- [5] Raheem, Z.; Kareem, A. A.: Wear and friction of polymer fiber composites coated by NiCr alloy. *Eng. Trans.* 65 (2017) 2, pp. 307–318.
<http://et.ippt.pan.pl/index.php/et/article/view/386>
- [6] Liu, A.; Guo, M.; Gao, J.; Zhao, M.: Influence of bond coat on shear adhesion strength of erosion and thermal resistant coating for carbon fiber reinforced thermosetting polyimide. *Surf. Coat. Technol.* 201 (2006) 6, pp. 2696–2700. doi: 10.1016/j.surfcoat.2006.05.012
- [7] Liu, A.; Guo, M.; Zhao, M.; Ma, H.; Hu, S.: Arc sprayed erosion-resistant coating for carbon fiber reinforced polymer matrix composite substrates. *Surf. Coat. Technol.* 200 (2006) 9, pp. 3073–3077. doi: 10.1016/j.surfcoat.2005.01.042
- [8] Wang, R.; Song, D.; Liu, W.; He, X.: Effect of arc spraying power on the microstructure and mechanical properties of Zn–Al coating deposited onto carbon fiber reinforced epoxy composites. *Appl. Surf. Sci.* 257 (2010) 1, pp. 203–209. doi: 10.1016/j.apsusc.2010.06.065
- [9] Ganesan, A.; Yamada, M.; Fukumoto, M.: The effect of CFRP surface treatment on the splat morphology and coating adhesion strength. *J. Therm. Spray Technol.* 23 (2014) 1–2, pp. 236–244. doi: 10.1007/s11666-013-0003-z

- [10] Belcher, M. A.; Wohl, C. J.; Hopkins, J. W.; Connell, J. W.: Laser surface preparation and bonding of aerospace structural composites, 2010.
<https://ntrs.nasa.gov/search.jsp?R=20100021129> (accessed 5 October 2021).
- [11] Li, S.; Sun, T.; Liu, C.; Yang, W.; Tang, Q.: A study of laser surface treatment in bonded repair of composite aircraft structures. *R. Soc. Open Sci.* 5 (2018) 3, 171272. doi: 10.1098/rsos.171272
- [12] Fischer, F.; Kreling, S.; Dilger, K.: Surface structuring of CFRP by using modern excimer laser sources. *Phys. Procedia* 39 (2012), pp. 154–160. doi: 10.1016/j.phpro.2012.10.025
- [13] Fischer, F.; Kreling, S.; Jäschke, P.; Frauenhofer, M.; Kracht, D.; Dilger, K.: Laser surface pre-treatment of CFRP for adhesive bonding in consideration of the absorption behaviour. *J. Adhes.* 88 (2012) 4–6, pp. 350–363. doi: 10.1080/00218464.2012.660042
- [14] Liebsch, A.; Koshukow, W.; Gebauer, J.; Kupfer, R.; Gude, M.: Overmoulding of consolidated fibre-reinforced thermoplastics - increasing the bonding strength by physical surface pre-treatments. *Procedia CIRP* 85 (2019), pp. 212–217. doi: 10.1016/j.procir.2019.09.047
- [15] Gebauer, J.; Franke, V.: Verfahren zur Herstellung eines Bauteils, das mit einem Faserverbundwerkstoff gebildet ist. Patent DE 10 2017 201 507 A1.
- [16] Gebauer, J.; Klotzbach, U.; Lasagni, A. F.: Functionalization of fiber-reinforced plastic based on laser micro structuring. In: Klotzbach, U.; Kling, R.; Watanabe, A. (Eds.). *Laser-based micro- and nanoprocessing XIII*. San Francisco, United States, 02.02.2019 - 07.02.2019, SPIE, 2019, p. 11.
<https://www.spiedigitallibrary.org/conference-proceedings-of-spie/10906/2505114/Functionalization-of-fiber-reinforced-plastic-based-on-laser-micro-structuring/10.1117/12.2505114.full>
- [17] Gebauer, J.; Paczkowski, G.; Weixler, J.; Klotzbach, U.: Cold surface treatments on fiber-reinforced plastics by pulsed laser. *Technologies for Lightweight Structures* 1 (2017) 2. doi: 10.21935/tls.v1i2.105
- [18] Gebauer, J.; Burkhardt, M.; Franke, V.; Lasagni, A. F.: On the ablation behavior of carbon fiber-reinforced plastics during laser surface treatment using pulsed lasers. *Materials* 13 (2020) 24, pp. 1–17, 5683, doi: 10.3390/ma13245682
- [19] Gustke, K.; Gebauer, J.; Drehmann, R.; Lasagni, A. F.; Lampke, T.: Enhancement of the adhesion of wire arc sprayed coatings on carbon fiber-reinforced plastic by surface laser structuring. *Coatings* 11 (2021) 4, 467. doi: 10.3390/coatings11040467